International Journal of Mechanical Sciences ▮ (▮▮▮▮) ▮▮▮–▮▮▮

Contents lists available at SciVerse ScienceDirect

International Journal of Mechanical Sciences

journal homepage: www.elsevier.com/locate/ijmecsci

Energy dissipation in a frictional incomplete contact with varying normal load

M. Davies [a,*,1], J.R. Barber [b], D.A. Hills [a]

[a] Department of Engineering Science, Oxford University, Parks Road, Oxford OX1 3PJ, United Kingdom
[b] Department of Mechanical Engineering and Applied Mechanics, University of Michigan, Ann Arbor, MI 48109-2125, USA

ARTICLE INFO

Article history:
Received 14 July 2011
Received in revised form
4 October 2011
Accepted 7 November 2011

Keywords:
Contact mechanics
Combined loading
Hertz
Fretting fatigue
Frictional contact
Half plane theory

ABSTRACT

The problem of a plane incomplete frictional contact, subject to a constant normal force, together with periodically varying tangential and additional normal forces, is studied. The evolution of the stick-slip patterns, together with the frictional energy dissipation, both pointwise and summed over the whole contact, is found for a wide range of load cases, for two example geometries. viz. a Hertzian contact and a contact having a central flat face and rounded edges. The results are useful both in determining the damping properties of the contact and in assessing the localisation of surface damage which may give rise to fretting damage and possible crack nucleation.

1. Introduction

Stationary contacts in mechanical assemblies are often subject to cyclically varying loads, usually caused by vibration. These almost invariably give rise to slip regions within the contact, even though the contact itself is far from the sliding condition. Within the context of contacts which are capable of idealisation using half-plane theory, the majority of the cases treated address the case when the normal load is held constant, and only the tangential force varies with time. A partial slip solution for the classic contact mechanics problem, the celebrated 'Hertz' problem [1] of contact between cylinders of equal radius, was devised by Cattaneo [2] and extended in a series of articles by Mindlin [3,4]. A review of these, and of the phenomenon of partial slip, is given by Deresiewicz [5]. More recent developments include taking into account the influence of remote tensions [6], and a generalisation of the procedure devised by Cattaneo and Mindlin to other geometries has been provided by Ciavarella [7] and independently, Jäger [8]. This has resulted in published solutions for a flat punch with rounded corners [9] and a punch composed of a curved central region with smaller edge radii [10].

Many real problems incorporating contacts do not experience quite this loading history, because the normal contact load is also affected. In a gas turbine, for example, 'running up' the engine generates a proportional combination of normal load/tangential load/differential tension on the rotor/blade contacts, whereas in flight these same contacts experience relatively high frequency vibration, which exhibits a ratio between these modes of loading varying in a much more complex way with time. Another, simple example is displayed in Fig. 1, which shows a motor resting on a contact which has a flat face but radiused edges, and subject to a constant normal self-weight. When the motor is run, well away from resonance conditions, the presence of any out-of-balance mass will develop a radial force constant in magnitude, but which has horizontal and vertical components which vary harmonically in time. The object of this article is to show, first, how the contact size and attendant slip regions evolve, and then to deduce the frictional energy dissipated, both in a pointwise and overall sense.

Recently, the authors developed a method for determining the evolution of stick and slip regimes for any contact capable of idealisation by an uncoupled half-plane model, and subject to loading in the form of closed loops in $P-Q$ space, when P is the contact normal load and Q the shear load [11]. The majority of the article was concerned with the deduction of the stick-slip regime as the loading was taken through a complete cycle, and the formulation was left at a completely general level, independent of the contact geometry. Here we shall use this procedure to

* Corresponding author.
E-mail addresses: mat.davies@eng.ox.ac.uk, mat.davies@rolls-royce.com (M. Davies).
[1] Also with Rolls-Royce plc, P.O. Box 31, Derby DE24 8BJ, United Kingdom.

0020-7403/$ - see front matter © 2011 Elsevier Ltd. All rights reserved.
doi:10.1016/j.ijmecsci.2011.11.006

investigate the effect of the loading cycle on the total frictional energy dissipation (hysteretic damping) during the cycle and on the location and magnitude of the maximum dissipation per unit area, which we expect to correlate with the initiation point for fretting fatigue. The method is illustrated first for a Hertzian geometry and then for a flat and rounded punch, but it can be readily extended to other cases. A Mathematica code has been developed for this purpose and will be freely available as accompanying material.

2. First and steady state cycles

The procedure for determining the traction distributions and stick-slip zone mix is given in full in [11], and that article should be consulted for full details. The philosophy is one of using a superposition of shearing tractions corresponding to scaled values of the normal load and hence extent of the contact, as the contact problem is taken from an unloaded state to a point on the loop, Fig. 2, and then around the loop. The first step is to establish the contact law relating the contact half-width, a, to the normal load, P, and a description of the contact pressure distribution $p(x,P)$.

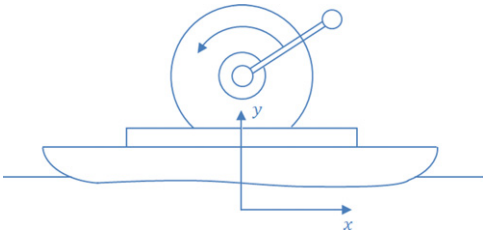

Fig. 1. Contact supporting a motor with an eccentric weight.

We introduce, also, the notation that the derivative of the contact pressure with respect to the normal load, P, is denoted by $p'(x,P)$—i.e.

$$p'(x,P) \equiv \frac{\partial p(x,P)}{\partial P}. \tag{1}$$

This compact notation enables us to write down solutions very simply; for example, the shear traction distribution for a stationary contact subject to a monotonically increasing shear (where the Hertz problem gives rise to the Cattaneo–Mindlin problem, but the solution as now written applies to any uncoupled half-plane problem [7,8]) is

$$q(x) = f[p(x,P) - p(x; Q-P)], \tag{2}$$

where f is the coefficient of friction and Q is the applied (increasing) shearing force. It is understood that the terms are evaluated only when the observation point falls within the contact corresponding to that particular load, so that, in the above expression, the second term contributes only when the observation point falls with the range where the same punch, subject to a normal load $Q-P$, forms a contact.

The assumed form of the loop is that it is elliptical with arbitrary phase angle, ϕ (chosen >0), so that the variation of the load with time, t, is given by

$$P(t) = P_0 + P_1 \cos(\omega t), \tag{3}$$

$$Q(t) = Q_0 + Q_1 \cos(\omega t - \phi), \tag{4}$$

and progression in time will track out in an anticlockwise sense. In order to reach the steady state cycle, we need to define a transient loading path such as the line OA in Fig. 2. In [7], we showed that the details of the trajectory OA affect only the shear

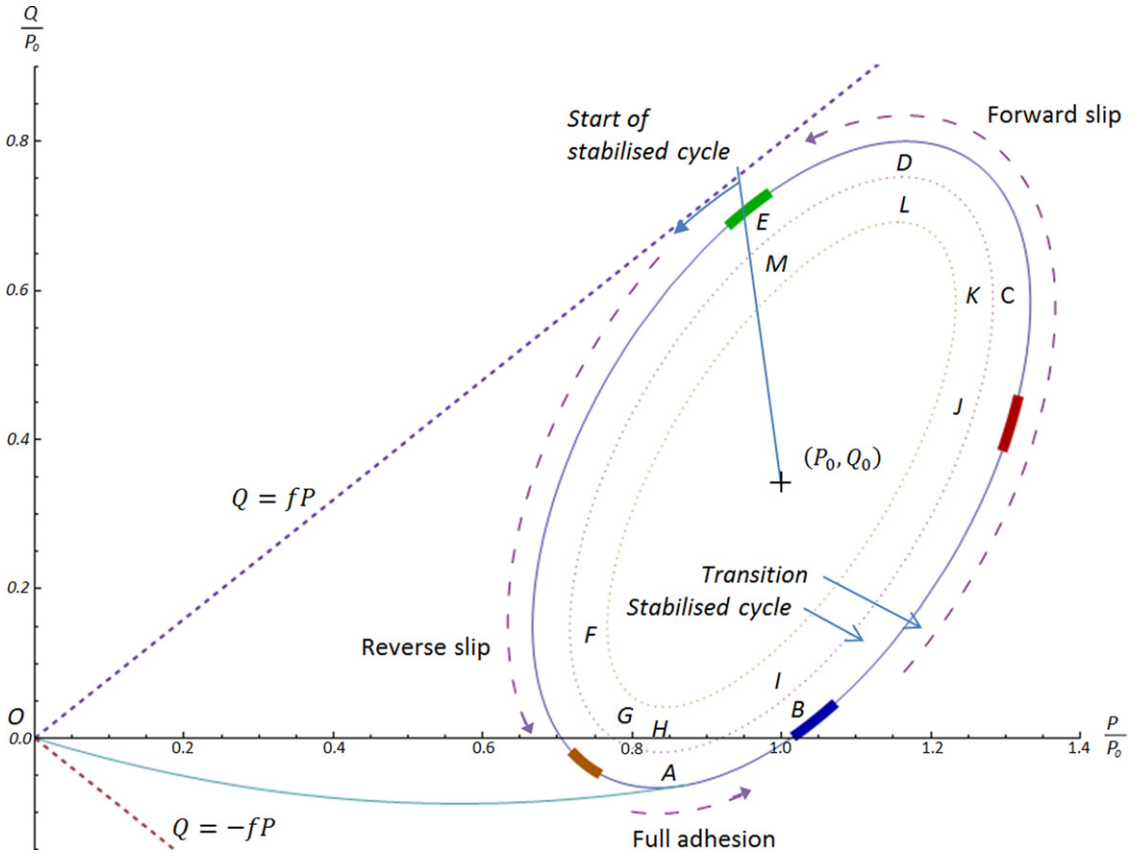

Fig. 2. Definition of load history.

Please cite this article as: Davies M, et al. Energy dissipation in a frictional incomplete contact with varying normal load. Int. J. Mech. Sci. (2012), doi:10.1016/j.ijmecsci.2011.11.006

tractions locked into the 'permanent stick zone' as will be shown later in this section, but have no effect on the extent of slip or the dissipation in the steady state. The detailed shape of this phase is therefore unimportant, but we choose a path satisfying the condition $dQ/dP < f$, for which stick endures throughout the transient Full stick persists not only during the transient, but until the loading point moves around to a point B, when $dQ/dP = f$. We have shown [11] that, for a general segment of loading trajectory, subject to an increasing normal load, with initial state (P_α, Q_α) and final state (P_β, Q_β) the change in traction is given by

$$q_\beta(x) = q_\alpha(x) + \int_{P_\alpha}^{P_\beta} p'(x,P)\frac{dQ}{dP}\,dP. \tag{5}$$

This may be used to establish the tractions first at the end of the transient loading ($P_\alpha = Q_\alpha = 0$, $P_\beta = P_A, Q_\beta = Q_A$) and through to an end point given by ($P_\beta = P_B, Q_\beta = Q_B$).

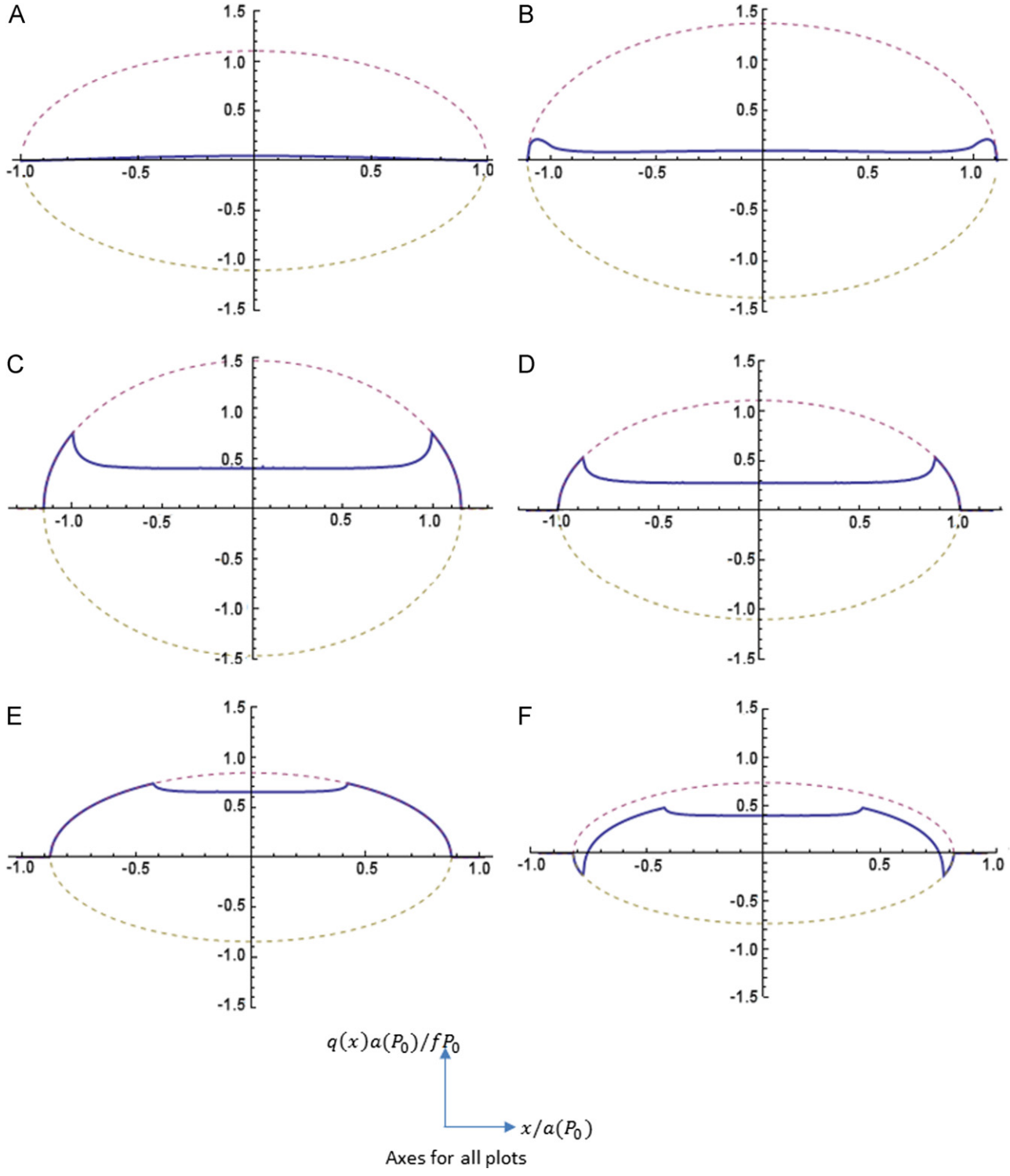

Fig. 3. Shear traction distribution beneath Hertzian contact at various stages in the load cycle.

Please cite this article as: Davies M, et al. Energy dissipation in a frictional incomplete contact with varying normal load. Int. J. Mech. Sci. (2012), doi:10.1016/j.ijmecsci.2011.11.006

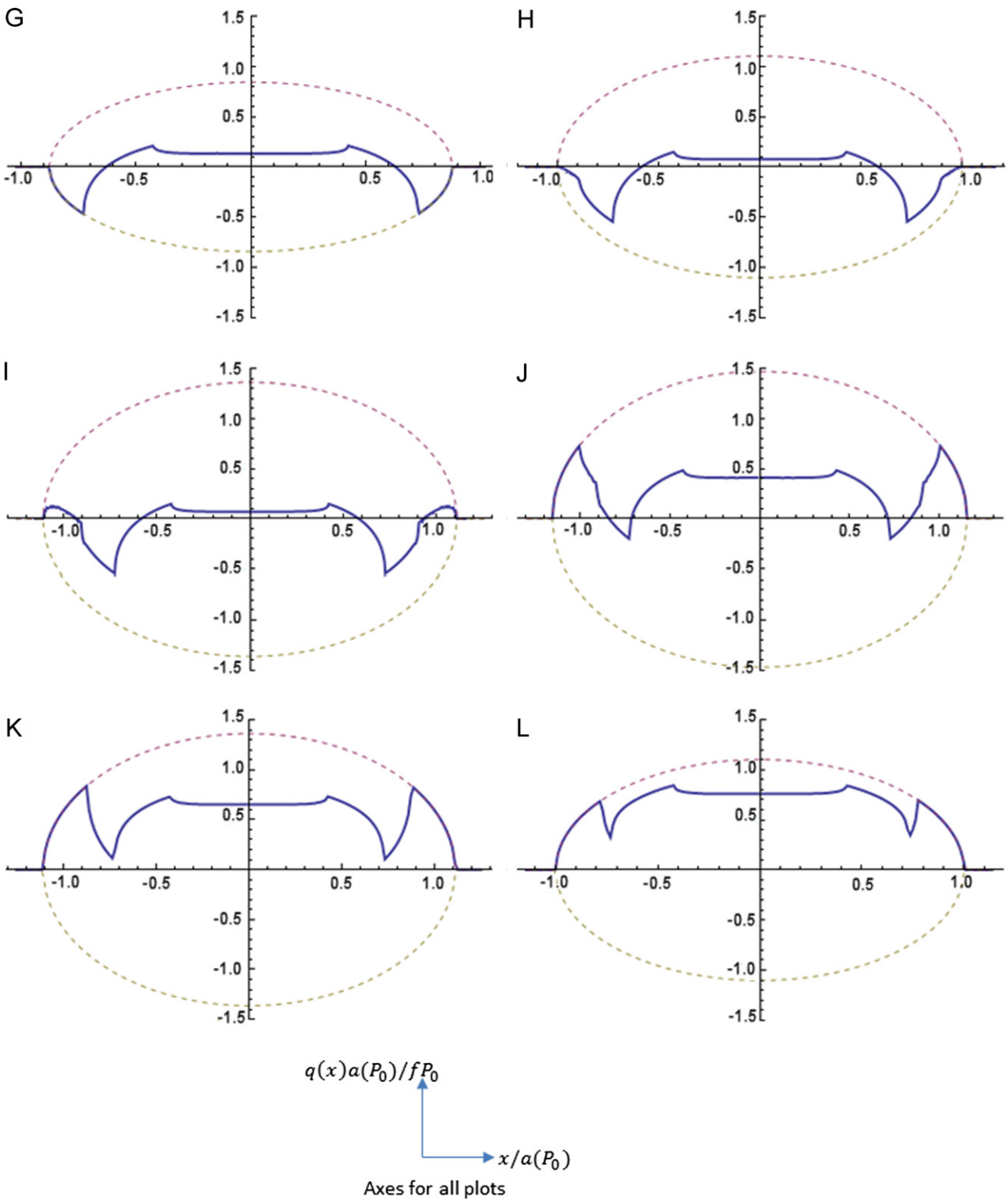

Fig. 3. (*continued*)

Although the theory presented in this section is general in the sense that it may be applied to a punch having any geometry capable of idealisation within the half-plane formulation, Fig. 3 shows, as an example, the evolving contact size, pressure distribution, and shear traction distribution during the whole load cycle, for a Hertzian contact, and should be read in conjunction with Fig. 2. Further details of the contact law and pressure distribution needed to achieve these results are given in Section 3.1. The x-coordinate is normalised with respect to the contact half width when the normal contact load is P_0, and this is also used to normalise the tractions. The example characteristics chosen are $P_0=3, Q_0=1.1, P_1=Q_1=1$, $\phi=\pi/2$ and $f=1.0$, which means that the ellipse plots out as a circle. The transient load path is assumed to be a parabola, blending smoothly with the ellipse describing the steady state problem at P_A. The letters on this figure correspond to those used on Fig. 2, and also, to those used on later figures. Note that A–D relate to the

Please cite this article as: Davies M, et al. Energy dissipation in a frictional incomplete contact with varying normal load. Int. J. Mech. Sci. (2012), doi:10.1016/j.ijmecsci.2011.11.006

transient behaviour displayed during the first cycle, and E to M relate to steady state behaviour. Fig. 3A and B shows, in particular, the shearing tractions while the contact remains adhered, during the transient response.

During the next phase of loading, forward slip regions, attached to the contact edges, develop and grow. The contact itself clearly initially gets bigger, up to point C, but then contracts. Note, though, that the stick slip boundaries recede continuously, so that the slip zone is formally advancing, right the way through to point E, when $dQ/dP=f$ (note $dP<0, dQ<0$). During this time, the traction distribution at a general point X has been shown to be given by

$$q_X(x)=\int_0^{P_Y} p'(x,P)\frac{dQ}{dP}dP+f(p(x,P_x)-p(x,P_Y)), \tag{6}$$

where the point Y is defined by a line drawn through X, of gradient f, and denotes the intersection of this line with the initial full stick trajectory. Fig. 3C–E shows the shearing traction during this phase – point C is the point where the maximum normal load occurs, Point D where the shear force reaches a maximum, and point E the maximum extent of forward slip. When point E is reached the whole contact sticks instantaneously, and then as we move further around the loop, a region of reverse slip develops, and the shear traction is given by

$$q(x)=\int_0^{P_Z} p'(x,P)\frac{dQ}{dP}dP+f(-p(x,P)+2p(x,P_S)-p(x,P_Z)), \tag{7}$$

where P_Z is the load on the initial loading line where a line of gradient f and passing through E intersects it, and P_S is given by

$$P_S=\frac{1}{2}\left(\frac{Q}{f}+P-\frac{Q_Z}{f}+P_Z\right). \tag{8}$$

In fact, this point represents the first stabilised solution on the steady state cycle. The shear tractions are defined by Eqs. (6) and (7) until we reach point G, where $dQ/dP=-f$. Fig. 3F, G depicts the shear traction in this regime – 3F when the normal load reaches its minimum value and point G the instant before full stick again occurs. These figures include the familiar 'hooks' observed in Cattaneo–Mindlin distributions at the point where forward slip reaches its maximum value and became locked in. At the point where full stick occurs (G) the shearing traction is, explicitly

$$q_G(x)=\int_0^{P_Z} p'(x,P)\frac{dQ}{dP}dP+f(-p(x,P_B)+2p(x,P_T)-p(x,P_Z)), \tag{9}$$

and the point T is

$$P_T=\frac{1}{2}\left(\frac{Q_B}{f}+P_B-\frac{Q_E}{f}+P_E\right). \tag{10}$$

During the second cycle of loading the general procedure remains the same, save that the locked in traction is now that established at point G, and that, when we carry out the constructions needed, the intersection is now with a point on the loop rather than the transient initial curve. For full details refer to the original article [7].

As point G is passed, with full adhesion, we observe that, as expected, the full contact remains adhered until point B is reached (denoted I in this cycle, because the tractions present within the stick zone are different). See Fig. 3H (where the normal load reaches is minimum value) and I. From then on we observe advancing slip zones, as in the first cycle, and denoted by J (where the tractions being erased change from full stick to incipient reverse slip, and is located by drawing a line through point G, of gradient f, and finding the point of intersection with the loop), K (maximum normal load), L (maximum shear load) and M (incipient stick, and corresponding to point E at the beginning of the cycle). The evolution of the stick and slip zones, together with the tractions and contact size all subsequently remain identical from cycle to cycle. As stated earlier, the procedure described in this section applies to any punch capable of idealisation within the half-plane formulation, although the traction distributions plotted in Fig. 3 relate to a Hertzian contact.

The maximum extent of slip occurs during the first cycle of loading, and the corresponding stick region has an extent defined by $a(P_Z)$. During the transient cycle, new residual interfacial shearing tractions are established within the range $a(P_Z)<x<a(P_T)$, and in the steady state, the extent of permanent stick is defined by $a(P_T)$. The only residual information from the transient which persists is the locked-in distribution of shearing tractions within the permanent stick region, whose extent corresponds to the contact given by a load of magnitude P_T—this has no practical bearing on the performance of the contact, and hence the fretting performance of the contact as a whole does not depend on the load history prior to entering the steady state loop.

3. Energy dissipation

The rate of doing frictional work, per unit area, is given by

$$\dot{W}=f\oint_{\text{slip region}} p(x)\dot{u}(x)\,dx. \tag{11}$$

A knowledge of the irreversible work done is useful for two reasons; first, if we determine the rate of doing frictional work per unit area and then integrate this quantity over a steady state loading cycle this will reveal how the work done per unit area and per cycle of loading varies with position. We will subsequently refer to this as the pointwise dissipation. It will clearly be zero within that part of the contact which is always adhered and it will also fall smoothly to zero at the edges of the contact at its maximum extent, because the contact pressure falls smoothly to zero at the contact edges—it must therefore take a maximum somewhere within the steady state slip zone and, as the damage done may sensibly be assumed to be directly controlled by the irreversible work, the maximum value (with respect to position), could be used as a simple first approximation of a crack nucleation parameter. The second quantity of interest is the integral of the pointwise dissipation with respect to position, which then gives us the total work done per cycle of loading, and hence gives a good measure of the damping provided by the contact when the excitation force is in the form of vibration. This will be referred to as the global dissipation. It has been shown [11] that, whilst the locked in shearing tractions within the stick region depend on the mean shear force, Q_1, the stick and slip zone distributions, and consequently the shearing tractions in the slip region, are independent of this quantity. Consequently, the work done against friction is also independent of the mean shearing force.

Note that, although the total forwards and backwards relative slip displacements of any pair of particles must be equal during the forward and reverse slip phases of the loading cycle, it does not follow that the work done in each phase of slip is the same, because the size of the contact, and hence the magnitude of the contact pressure, may not be the same at corresponding slip zone extents. Any slip occurring within the portion of the contact that remains in contact for the entire cycle will have to be identical in the forward and reverse slip regions, which can be written as

$$\oint_{P_E}^{P_M} \dot{u}(x,P)\,dP=0. \tag{12}$$

We first turn our attention to the incremental slip displacement associated with the incremental tangential traction, given by

$$Cfp'(x,P_1)\Delta P, \tag{13}$$

where P_1 refers to the load on the 'corrective punch' and applies within the stick region. The constant (for this segment of loading

Please cite this article as: Davies M, et al. Energy dissipation in a frictional incomplete contact with varying normal load. Int. J. Mech. Sci. (2012), doi:10.1016/j.ijmecsci.2011.11.006

history), C, is the multiplier on the incremental traction in each region and takes the following values around the stabilised cycle (see Fig. 2)

$$C=\begin{cases}\dfrac{1}{f}\dfrac{dQ}{dP}+1 & \text{in } EG,\\ \dfrac{1}{f}\dfrac{dQ}{dP}(P_Y)-1 & \text{in } IJ,\\ \dfrac{1}{f}\dfrac{dQ}{dP}-1 & \text{in } JM.\end{cases} \tag{14}$$

No slip, and hence, no frictional dissipation occurs in GI. In a second recent paper [12] extensive notes on the evaluation of locked-in surface displacements and their variation with the corresponding shear traction was undertaken and we showed that the duality between the normal and shear tangential displacement governing equations enables us to write:

$$\Delta u(x)=Cf\Delta P\frac{(1+\kappa)}{2\pi\mu}\int_c^x h_o(x,c)\,dx, \tag{15}$$

where $h_o(x)$ is the function describing the initial gap between punch and half-plane. This means that:

1. In EG

$$\begin{aligned}\Delta u&=\frac{f\Delta P(1+\kappa)}{\pi\mu}\frac{dP_S}{dP}\int_c^x\frac{dx}{\sqrt{x^2-c^2}} \quad c<x<a\\ &=\frac{f\Delta P(1+\kappa)}{\pi\mu}\frac{dP_S}{dP}\int_c^x\frac{dx}{\sqrt{x^2-c^2}}-\frac{f\Delta P(1+\kappa)}{2\pi\mu}\int_a^x\frac{dx}{\sqrt{x^2-c^2}} \quad a<x.\end{aligned} \tag{16}$$

2. In GI

$$\Delta u=\frac{f\Delta P(1+\kappa)}{\pi\mu}\frac{dQ}{dP}\int_a^x\frac{dx}{\sqrt{x^2-a^2}} \quad a<x. \tag{17}$$

3. In IJ

$$\begin{aligned}\Delta u&=\frac{\Delta P(1+\kappa)}{2\pi\mu}\left(\frac{dQ}{dP}P_Y\right)-f\frac{dP_Y}{dP}\int_c^x\frac{dx}{\sqrt{x^2-c^2}} \quad c<x<a\\ &=\frac{\Delta P(1+\kappa)}{2\pi\mu}\left(\frac{dQ}{dP}P_Y\right)-f\frac{dP_Y}{dP}\int_c^x\frac{dx}{\sqrt{x^2-c^2}}\\ &\quad+\frac{f\Delta P(1+\kappa)}{2\pi\mu}\int_a^x\frac{dx}{\sqrt{x^2-a^2}} \quad a<x.\end{aligned} \tag{18}$$

4. In JM

$$\begin{aligned}\Delta u&=-\frac{f\Delta P(1+\kappa)}{\pi\mu}\frac{dP_K}{dP}\int_c^x\frac{dx}{\sqrt{x^2-c^2}} \quad c<x<a\\ &=-\frac{f\Delta P(1+\kappa)}{\pi\mu}\frac{dP_K}{dP}\int_c^x\frac{dx}{\sqrt{x^2-c^2}}\\ &\quad+\frac{f\Delta P(1+\kappa)}{2\pi\mu}\int_a^x\frac{dx}{\sqrt{x^2-c^2}} \quad a<x.\end{aligned} \tag{19}$$

Note that, in all cases

$$\Delta u=0 \quad x<c. \tag{20}$$

Up to this point the expressions for energy expenditure are completely general, and we now look in detail at two specific examples.

4. Example

4.1. Hertzian punch

For a Hertzian contact between elastically similar materials, and where the relative radius of contact is R, the contact law and pressure distribution take the forms:

$$a(P)=\sqrt{\frac{PR(1+\kappa)}{\mu\pi}}, \tag{21}$$

$$p(x,P)=\frac{2\mu}{R(1+\kappa)}\sqrt{a(P)^2-x^2} \quad |x|<a(P)=0 \quad |x|>a(P). \tag{22}$$

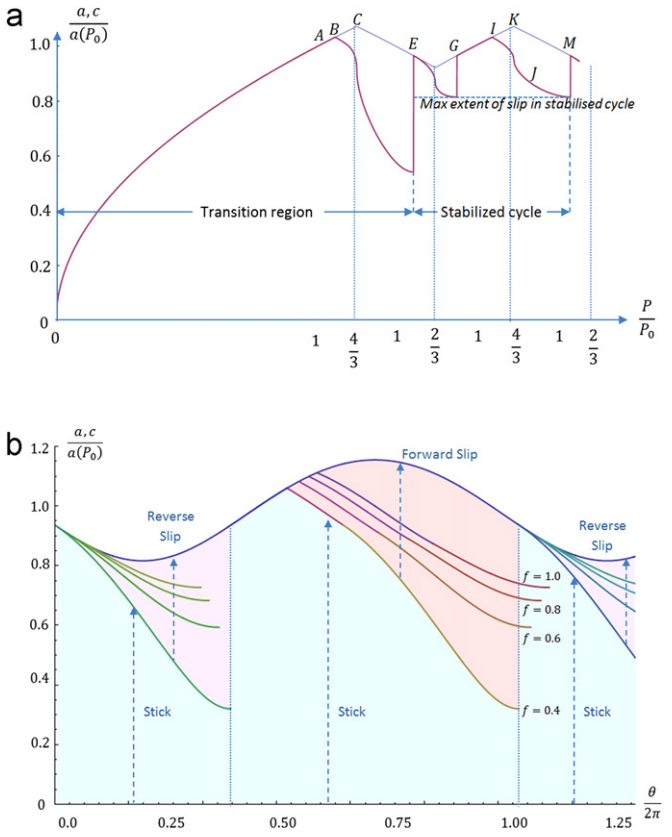

Fig. 4. (a) Contact size and stick zone size through cycle for Hertzian contact. (b) Contact size and extent of slip zone during stabilised cycle for various values of friction.

Fig. 3 has already been introduced, primarily to illustrate the procedure developed, and here we first re-examine it in order to provide more details of the results themselves. Fig. 3 implicitly gives the size of the contact and extent of slip as snapshots through the cycle, but a fuller picture is provided in Fig. 4(a). The abscissa gives the progression of load, and note that this means that the axis is slightly unusual, increasing monotonically up to point C, but then alternately decreasing (to point F) and increasing again back to point K. On the ordinate we show, for half of the contact, its size ($a(P)/a(P_0)$), and the size of the stick region ($c(P)/a(P_0)$). This clearly shows that the slip zone is much bigger during the transient first cycle (points B–E) than it is during the steady state (the second cycle, regions I–M). It also shows that, in the steady state, the extent of slip penetration from the contact edges is the same during forward and reverse slip, although, of course, the contact spends a bigger fraction of the time undergoing forwards slip than reverse slip; it follows that, because the net slip of a particle around a loading cycle must be zero, the mean forward slip velocity is lower than the magnitude of the mean reverse slip velocity. The contact is always fully adhered during the interval G–I.

The same information, for the steady state, is re-plotted in Fig. 4(b). This time, though, we denote progress around the cycle by the angle θ ($=\omega(t-t_M)$), so that it is measured from point M,

Please cite this article as: Davies M, et al. Energy dissipation in a frictional incomplete contact with varying normal load. Int. J. Mech. Sci. (2012), doi:10.1016/j.ijmecsci.2011.11.006

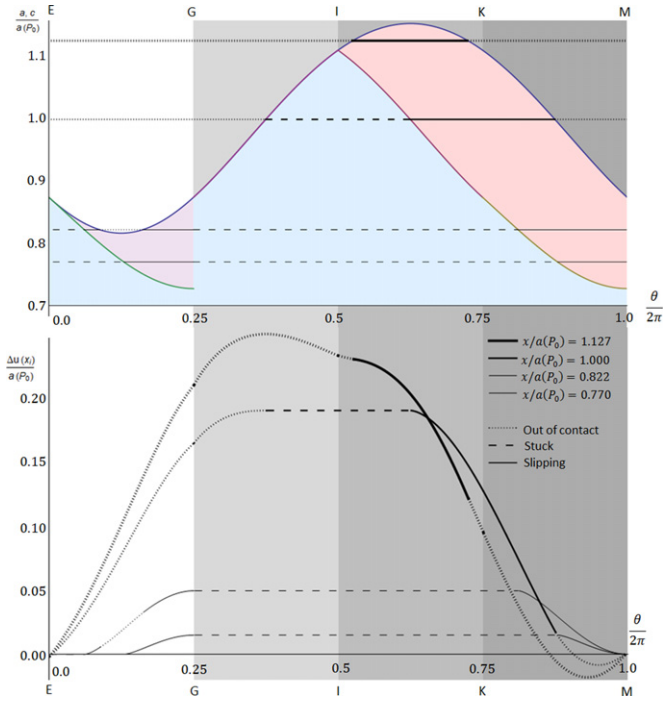

Fig. 5. Stick-slip-out of contact and displacement stabilized cycle history plot for four points beneath a Hertz contact.

the first point on the steady state cycle, in Fig. 2. The different implied definition of normal load means that the size of the contact now appears as a harmonic function, and the figure also summarises the extent of slip for $f = 1.0,0.8,0.6,0.4$. Note that the change of shading has been used to emphasize the slip-stick transition points for the case of $f=0.4$, and for higher coefficients of friction the transition is delayed.

It is illuminating, at this point, to study the relative tangential displacement of pairs of corresponding surface particles in more detail. We again employ a coefficient of friction of 1.0 as in the example treated in Figs. 3 and 4(a), and plot out, in the upper part of Fig. 5, the evolution of the contact extent and slip extent as a function of the angular position, θ, around the loop. This figure again includes the letters from Fig. 2, showing the progression of the load history. Also marked on this figure are four locations in the contact, at $x/a(P_0) = 0.77,0.82,1.0,1.13$. Thus, as will be clear, the first of these $(x/a(P_0) = 0.77)$ is always in contact, and experiences a sequence – stick, reverse slip,stick, forwards slip, the second $(x/a(P_0) = 0.82)$ leaves contact for only a very short period during the cycle and experiences – stick, reverse slip, separation, reverse slip,stick, forwards slip. The third point $(x/a(P_0) = 1.0)$ experiences an increased period of separation, with an overall history – separation,stick, forwards slip separation, and lastly, the fourth point $(x/a(P_0) = 1.13)$ sees a history – separation, forwards slip, separation. Using formulae (16)–(19) the relative tangential displacement of opposing points at these positions were tracked out over the cycle, and the results are shown in the lower part of Fig. 5. There can, of course, be no net displacement over the load cycle for any pair of opposed points equation (11), but the diagram makes it clear that part of the displacement in one sense occurs when the surfaces are separated, so that the fretting, for points remote from the contact centre $(x/a(P_0) \gtrsim 0.88)$ occurs exclusively in one direction. We might therefore expect the surface damage in such cases to display rather different characteristics from those apparent after a Cattaneo-type test, where contact damage is fully reversing at all points.

We now look in more detail at the energy expenditure. For a Hertz contact, Eq. (12) becomes

$$\dot{u}(x) = -Cf\Delta P\frac{(1+\kappa)}{2\pi\mu}\cosh^{-1}\frac{x}{c}, \tag{23}$$

and the pointwise dissipation at a given position, x, is

$$W(x) = -\frac{f^2}{\pi R}\int_{P_E}^{P_M}\sqrt{a(P)^2 - x^2}C\,\cosh^{-1}\left(\frac{x}{c}\right)dP, \tag{24}$$

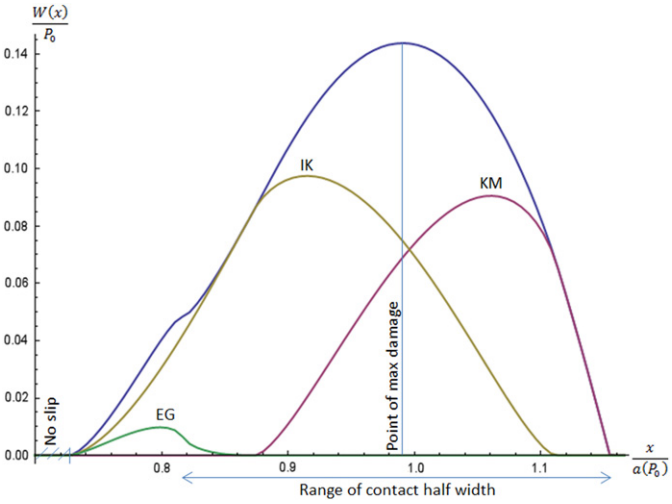

Fig. 6. Pointwise dissipation for a Hertzian contact.

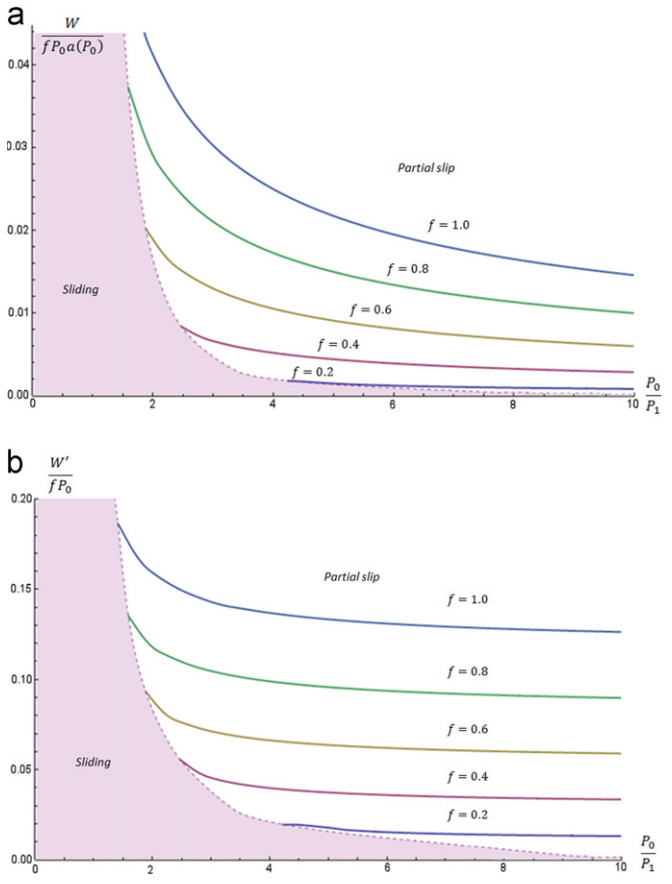

Fig. 7. (a) Global dissipation experienced by a Hertzian contact during one cycle of load. (b) Peak pointwise dissipation experienced by a Hertzian contact during one cycle of load.

Please cite this article as: Davies M, et al. Energy dissipation in a frictional incomplete contact with varying normal load. Int. J. Mech. Sci. (2012), doi:10.1016/j.ijmecsci.2011.11.006

where P_E and P_M specify the same location on the loading trajectory, separated by one complete revolution, as shown in Fig. 2. The remainder of the problem must be handled numerically. For the example problem looked at in detail above (Figs. 4(a) and 5), the variation of pointwise dissipation with position per cycle of load is shown in Fig. 6. This makes it clear that the vast majority of the frictional work is expended during the forward slip phases (*IJ* and *JM*) and very little during reverse slip (EG), and reflects the fact that the contact pressure at any given point is rather higher during the forward slip phase than it is during reverse slip. The highest point on the figure represents the position within the contact where the pointwise dissipation is greatest. At the transition point from permanent steady state stick ($x/a \simeq 0.73$) the curves have zero slope, whereas at the at the outer edge of the contact they have a finite slope (and an approximately square root bounded characteristic), so that the location of the maximum is pushed outwards from the centre of the slip range; for this case the maximum is located at just over 60% of the distance from the permanent steady state stick point to the maximum contact half-width.

A further integration, along the slip zones gives the global dissipation, during one cycle. The results of a number of calculations such as these, for various coefficients of friction, and for various values of P_1/P_0 (and $Q_1 = P_1$), are shown in Fig. 7. Fig. 7(a) shows the global dissipation, and therefore effectively provides information about damping. As might be expected, for a given coefficient of friction the maximum energy dissipated occurs just before the sliding condition is encountered. Given that the values chosen for P_1, Q_1 and ϕ specify a circle the boundary defining sliding – when the ellipse in Fig. 2 lies on the x-axis (i.e. $Q_0 = 0$) is just about to touch the sliding line – is given by

$$\frac{P_0}{P_1} > \frac{\sqrt{2}(1+f)}{2f}. \tag{25}$$

Fig. 7(b) on the other hand, gives the pointwise dissipation per cycle at the maximum position within the contact as a function of P_0/P_1 and f. Again the damage done is severest when we have incipient sliding, but it will be noted that the damping (total) energy falls off much more quickly than the peak value as the value P_0 is increased. It follows that the best designs – in the sense that the ratio of damping energy to localised energy is maximised – occur when the locus is close to the sliding condition.

4.2. Flat and rounded punch

The calculations carried out above for the Hertzian contact have been executed, also, for a punch having a 'flat and rounded' profile, i.e. one where the punch face has a central flat region of half-length b, bordered by edge radii R which smoothly blend with the flat face. For this case the contact law may not be defined in closed form [9] and the contact half-width, a, is given by

$$\frac{PR(1+\kappa)}{4a^2\mu} = \frac{\pi - 2\phi_0}{4\sin^2\phi_0} - \frac{\cot\phi_0}{2}, \quad \text{where}$$

$$\sin\phi_0 = \frac{b}{a},$$

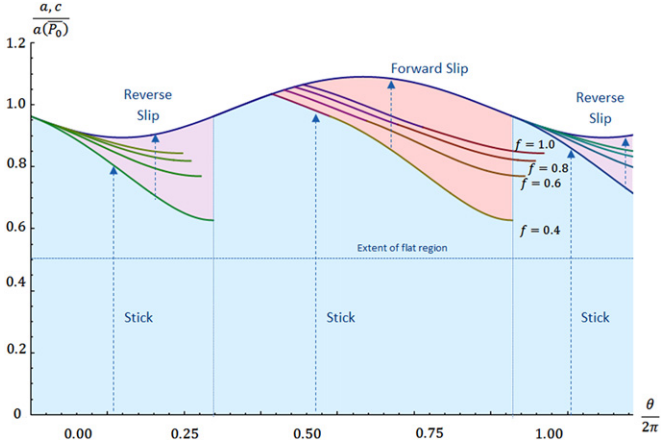

Fig. 8. Variation of a and c for flat and rounded contact ($b/a(\overline{P}) = 0.505$).

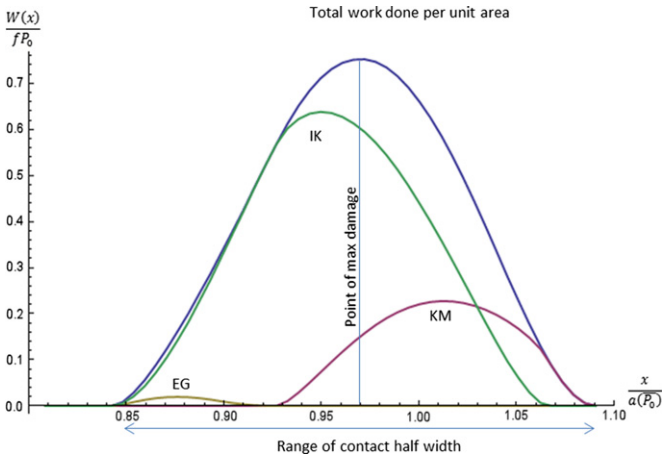

Fig. 9. Pointwise dissipation for a flat and rounded contact ($b/a(\overline{P}) = 0.505$).

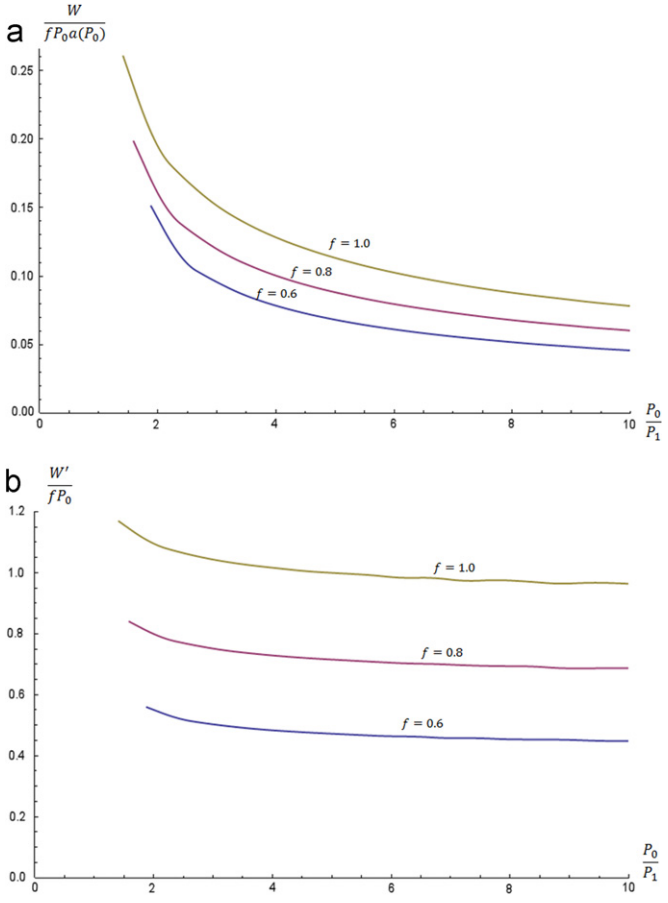

Fig. 10. (a) Global dissipation experienced by a flat and rounded contact during one cycle of load ($b/a(\overline{P}) = 0.505$). (b) Peak pointwise dissipation experienced by a flat and rounded contact during one cycle of load ($b/a(\overline{P}) = 0.505$).

Please cite this article as: Davies M, et al. Energy dissipation in a frictional incomplete contact with varying normal load. Int. J. Mech. Sci. (2012), doi:10.1016/j.ijmecsci.2011.11.006

and the contact pressure is itself rather complicated, so much of the evaluation has to be done numerically. There are clearly several combinations of applied normal load and edge radius which will give rise to the same contact width, but the properties of the solution are really dictated by the ratio b/a, so as an example geometry we choose $b/a(P_0)=0.505$ where $a(P_0)$ is the contact width at the mean normal load. The geometry was then subjected to exactly the same load history as the Hertz case, defined by $P_0=3, Q_0=1.1, P_1=Q_1=1$, $\phi=\pi/2$ and $f=1.0$.

For this geometry the evolution of the contact size and the evolution of the stick zone with load around the loading cycle are shown in Fig. 8. In the absence of tension the extent of slip must be confined to the radiused regions for problems of this kind, but the overall form of Fig. 8 is quite similar to the hertz result displayed in Fig. 4(b). The principal effect of introducing the flat region is therefore simply to localise slip in two bands at the edges of the contact. Fig. 9 shows the pointwise dissipation for the problem, which is again similar in form to the Hertz result shown in Fig. 6, except that, again, all of the dissipation arises in the edge radii, and we note that, as before, the peak occurs at a point about 60% of the way to the contact edge measured from the edge of the stick/slip boundary. More interesting are the results for the dissipation shown in Fig. 10, which may be compared with Fig. 7 for the Hertz case. Fig. 10(a) shows the global dissipation, and this is similar in form to the Hertz case, but, with the normalisation as shown, about fives times as much energy absorbed for a given coefficient of friction and amplitude of oscillatory load. In the case of the peak pointwise dissipation, the curves for the flat and rounded indenter show a weaker dependence of the peak value on the ratio $P_1/P_0=Q_1/P_0$, and generally the value is of order eight times that for Hertz. If a figure of merit is the ratio of global dissipation to peak pointwise dissipation, for a given load, contact overall width and coefficient of friction, therefore, the Hertz geometry is preferable to, at least, the sample flat and rounded punch examined. Qualitatively, it may be seen that this is because, in the case of the punch have a partly flat face, the slip region is itself localised, and hence is rather 'peakier' than the Hertz problem.

5. Concluding remarks

The paper shows, in detail, how the surface tractions, contact size and stick zone size evolve for any frictional contact capable of idealisation by uncoupled half-plane theory, and where the loading is oscillatory in both the normal and shear directions. It displays explicitly results derived in a recent paper, and is of practical relevance because many contacts practically exhibit this kind of loading history. two geometries are studied – a Hertz case, which permits some of the calculation to be done in closed form, and a flat punch with rounded edges; the latter was chosen so that roughly half of the contact lay in the flat region. Detailed information about the evolution of the stick slip pattern regime over a loading cycle is found, and from this we are able to deduce the frictional energy expended. This is done in two forms; an integral over the loading cycle which shows how the energy expended is localised (the pointwise dissipation) and a second one where this quantity is also integrated over the contact half width, effectively to provide the damping factor (the global dissipation). The location of the point of peak pointwise dissipation is found and, for the two geometries studied, is found to be located at a point just over 60% of the way from the stick-slip boundary to the contact edge. The introduction of a flat region means that the slip zones (in the absence of remote tension) are pushed outwards into the radiused edge regions, and this localisation means that the fretting performance, as measured by the pointwise dissipation parameter, becomes relatively worse compared with the damping performance, as measured by the global dissipation parameter.

A Mathematica file is available as supplementary information.

Appendix A. Supporting information

Supplementary data associated with this article can be found in the online version at doi:10.1016/j.ijmecsci.2011.11.006.

References

[1] Hertz H. Über die berührung fester elastischer Körper. J. Reine Angew. Math. 1882;92.
[2] Cattaneo C. Sul contatto di due corpi elastici: distribuzione locale degli sforzi. Rend dell'Accad Naz dei Lincei 1938;27:342–8. 434–436, 474–478 [in Italian].
[3] Mindlin RD. Compliance of elastic bodies in contact. ASME J Appl Mech 1949;16:259–68.
[4] Mindlin RD, Deresiewicz H. Elastic spheres in contact under varying oblique forces. ASME J Appl Mech 1953;75:327–44.
[5] Deresiewicz H. Bodies in contact with applications to granular media, in: Herrmann G. (Ed.), R.D. Mindlin and applied contact mechanics, Pergamon; 1974. p. 105–47.
[6] Hills DA, Nowell D. Mechanics of fretting fatigue tests. Int J Mech Sci 1986;29:355–65.
[7] Ciavarella M. The generalized Cattaneo partial slip plane contact problem. I-Theory, II Examples. Int J Solids Struct 1998;35:2349–78.
[8] Jäger J. A new principle in contact mechanics. ASME J Tribol 1998;120: 677–84.
[9] Ciavarella M, Hills DA, Monno G. The influence of rounded edges on indentation by a flat punch. Proc Inst Mech Eng part C. 1998;212:319–28.
[10] Vázquez J, Sackfield A, Hills DA, Domínguez J. The mechanical behaviour of a symmetrical punch with compound curvature. J Strain Anal 2010;45:209–22.
[11] Barber JR, Davies M, Hills DA. Frictional elastic contact with periodic loading. Int J Solids Struct 2011;48:2041–7.
[12] Hills DA, Davies M, Barber JR. An incremental formulation for half-plane contact problems subject to varying normal load, shear and tension. J Strain Anal 2011;45:436–43.

Please cite this article as: Davies M, et al. Energy dissipation in a frictional incomplete contact with varying normal load. Int. J. Mech. Sci. (2012), doi:10.1016/j.ijmecsci.2011.11.006